Analysis of auroral morphology: Substorm precursor and onset on January 10, 1997

G. A. Germany,[1] G. K. Parks,[2] H. Ranganath,[3] R. Elsen,[2] P. G. Richards,[3] W. Swift,[1] J. F. Spann,[4] M. Brittnacher [2]

Abstract. We study the dynamics of the poleward and equatorward boundaries of the auroral oval in response to the solar wind IMF on January 10, 1997 using global auroral images obtained by the Ultraviolet Imager (UVI) on Polar. A neural network algorithm is used to perform an automated morphological analysis. Poleward and equatorward boundaries identified by the algorithm exhibit clear equatorward motion during the substorm growth phase associated with the southward turning of the IMF. At substorm expansive phase onset, the high latitude edge of the oval expands poleward while the low latitude edge in the midnight sector shows continued expansion for several minutes after onset.

Introduction

The auroral oval boundaries are dynamic and, like the discrete auroral activity that are occurring in the oval, the boundaries expand and contract in response to geomagnetic and solar wind activities. Understanding the details of the oval boundary locations and dynamics is important because they can potentially reveal detailed information in the way the solar wind interacts with the geomagnetic field.

Previous study of the polar cap dynamics by *Frank and Craven* [1988] used a 1 kR threshold to define the polar cap boundary. Similar studies have also been performed using Viking images [e.g. *Murphree et al.*, 1991] *Makita et al.* [1985] and *Akasofu et al.* [1992] used observations of auroral electron precipitation from the DMSP satellite to infer the polar cap size. Ground observations of 630.0 nm auroral emissions at the polar cap boundary have also been used to estimate the polar cap boundary [*Blanchard et al.*, 1997]. Groundbased observations are restricted to nighttime visible observations within the local time sector of the observing station while *in situ* observations are limited to the satellite track.

Current imaging missions, as exemplified by the Ultraviolet Imager (UVI) on POLAR, are capable of high temporal resolution while viewing the entire auroral region. The UVI temporal resolution in normal operations is 36 seconds per frame. The POLAR apogee near 9 earth radii permits UVI to observe the entire auroral morphology for periods that can exceed 10 hours.

The purpose of this article is to use the Ultraviolet Imager observations made during the magnetic cloud event of January 10,

[1]Center for Space Plasma and Aeronomic Research, University of Alabama in Huntsville, Huntsville, AL.
[2]Geophysics Department, University of Washington, Seattle, WA.
[3]Computer Science Department, University of Alabama in Huntsville, AL.
[4]NASA Marshall Space Flight Center, Huntsville, AL.

1997 to study the spatial and temporal development of both polar cap and auroral oval areas. We show how the auroral activities in the polar cap region distorted and changed the polar cap boundary and also examine the dramatic changes of the oval shape that accompanied the growth phase activity. The boundaries identified in this study are based solely on observed emissions without comparison with *in situ* particle measurements, e.g. *Blanchard et al.* [1997]. Consequently, it is not certain from this study alone how well the UV emissions correlate with boundaries determined from particle precipitation characteristics. This is of particular concern for the poleward boundary determination where the particle precipitation can be weak. Comparison with precipitation data will be the subject of a future study.

Technique

Morphological analysis implicitly assumes that the region of active auroral processes is readily discernable from observation. This can often be difficult to automate as part of a production routine for auroral images, even though human observers can easily identify the auroral regions. While some work has been done with pattern recognition techniques with particle precipitation data [e.g. *Newell et al.*, 1991] there has not been comparable success with optical emissions as seen from auroral imagers. Consequently, auroral image analysis typically depends on interactive input to identify regions of interest in the image data. This represents a severe operational bottleneck, especially when the large number of images available with current imagers is considered (over 1.5 million for the Ultraviolet Imager to date). This study employs a new algorithm, based on neural network technology, to perform automated analysis of auroral morphology.

Pulse coupled neural networks (PCNN) have received considerable attention from the image processing community. If a digital image is applied as input to a pulse coupled neural network, the network groups image pixels based on spatial proximity and brightness similarity. During grouping, the network bridges small spatial gaps and minor local intensity variations. This is a very desirable property for image processing applications. The Pulse Coupled Neuron (PCN) model used here was developed by *Ranganath and Kuntimad* [1994] for image processing applications.

The PCN model analyzes the auroral image and provides a binary mask denoting which pixels lie within the auroral region. This mask is then used to estimate boundaries and areas within the oval region. A full analysis of the boundaries and regional areas, presented here, obviously requires a knowledge of spacecraft location and look direction. However, such information is not used to determine the image masks.

Boundaries were estimated for 1 hour local time sectors by examining a normalized probability distribution in magnetic latitude. The boundaries are chosen as the point where the probability distribution drops below a threshold value, here 33%

of the peak value of the distribution. In sectors where no auroral emissions are identified by the PCN model the boundaries are estimated by a polynomial fit to the existing boundary values. Areas are explicitly calculated for each image pixel in the identified region of interest and summed for total areas of both the auroral oval and the region of poleward of the oval, referred to below simply as the polar cap.

Data and Results

The Ultraviolet Imager has a spectral bandpass between 120 and 200 nm [*Torr et al.,* 1995]. In this study, image data taken with the LBHl filter (160 - 180 nm) is analyzed for auroral boundary estimation. This choice of filter has a number of advantages, including the fact that this wavelength range has negligible losses from O_2 absorption. The images thus include all emissions produced by precipitation energies up to several tens of keV and morphologies derived from the images are unaffected by changes in incident energy. Typical low level detection limits with this filter are between 50 and 100 Ry. The UVI far ultraviolet passband allows both dayside and nightside viewing which permits use of this technique under conditions not accessible to groundbased optical observations or visible imaging from space.

The UVI observations between 0100 and 0400 UT on January 10, 1997 have been discussed in detail by *Spann et al.* [1997]. The observations can be divided into three distinct periods: 1) initial encounter with the leading edge of the magnetic cloud (0057 - 0217 UT), 2) period of multiple sun-aligned arcs (0220 - 0257 UT), and 3) growth phase and substorm onset (0259 - 0401 UT). Image data taken between 0115 and 0418 UT were processed with the PCN algorithm to estimate the location of auroral emissions. For operational reasons, UVI images are taken with both 18 and 36 second exposures. For convenience, this study uses only 36 second exposures though the PCN works well with both exposures. The selection of LBHl images with 36 second exposures results in a 3 minute temporal resolution for this study.

Using the PCN image masks, the poleward and equatorward boundaries were determined for 1 hour bins in magnetic local time for each available image between 0100 and 0430 UT. Figure 1 shows these boundaries for 03, 06, 18, 21, and 24 MLT which frame the midnight sector. The period of time between 0200 and 0300 UT is dominated by the development of transpolar arcs (marked by arrows in the figure). These structures distort the poleward boundary estimates at these times, particularly in the 03 and 24 MLT sectors. The 24 MLT poleward boundary also shows a movement to higher latitudes prior to the transpolar arc development. However, this is due to a midnight intensification that began near 0125 UT and which was shown by *Spann et al.* [1997] to be the location from which the arc development began. Note that the expansion of the poleward boundary prior to 0200 UT is seen only in the 24 MLT sector where the intensification is located. This expansion occurred after the arrival of the solar wind pressure pulse and coincides with the initial development of the transpolar arcs.

The substorm growth phase from 0230 to 0334 UT is clearly seen in both the equatorward and poleward boundaries in the 24 MLT sector. The equatorward boundary advances from 67 to 62 degrees magnetic latitude during the growth period and continues advancing to 60 degrees in the 15 minutes after substorm onset at 0334 UT. The poleward boundary moves from 79 to 67 degrees at the same time. The growth phase is also seen in the 03 and 21 MLT sectors of both boundaries.
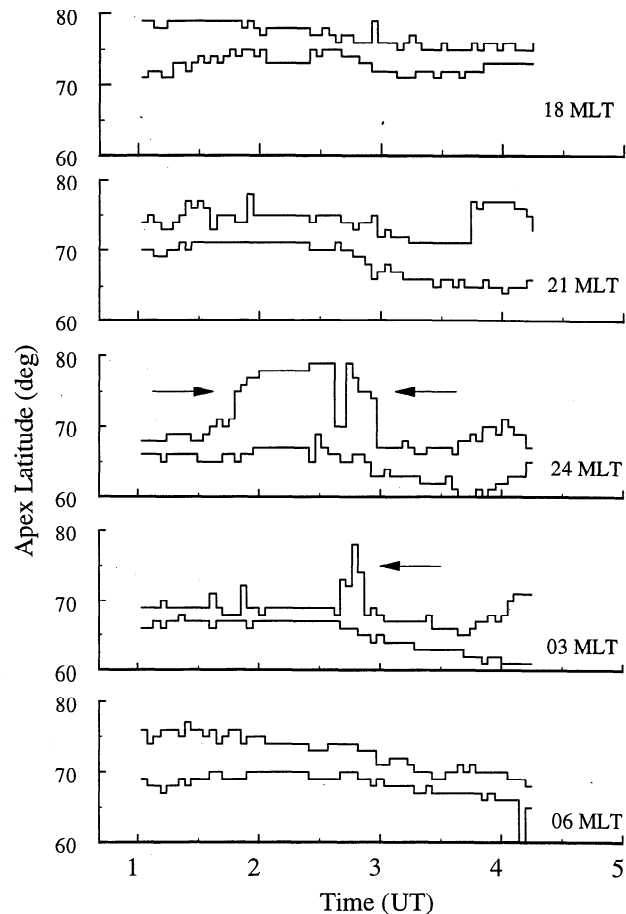

Figure 1. Equatorward and poleward boundaries derived from image masks. Boundaries are shown for 5 local times: 03, 06, 18, 21, and 24 MLT. The region between 2.5 and 3.0 UT is dominated by transpolar arcs that distort the boundary determinations during this period. The substorm growth phase is seen primarily in the postmidnight sector (24 - 03 MLT). Substorm onset is indicated by increase of poleward boundaries near 3.75 UT.

The substorm onset at 0334 UT is seen in the northward expansion of the poleward boundary as seen in the 21, 24, and 03 MLT data. The dusk/dawn boundaries at 06 and 18 MLT show little response to either the substorm growth phase or the initial substorm onset. This behavior is consistent with the observations reported by *Kamide et al.* [1997], who show that while poleward motion is observed in the midnight sector to begin at substorm onset, poleward motion of the dawn and dusk oval does not always occur at substorm onset and the motion may actually be equatorward for several minutes after onset on occasion.

Instead of analyzing 1 hour MLT bins as shown in Figure 1, it is also possible to perform a boundary analysis for the entire midnight sector (21 - 03 MLT) which is shown in Figure 2. The arcs prior to 0300 UT distort the poleward boundaries but the equatorward boundary estimates are basically unaffected. The substorm growth phase is clearly seen after 0230 UT, as is the northward expansion of the poleward boundary after 0334 UT. The equatorward boundary also shows some northward motion after 0334 UT but it is not as significant as for the poleward boundary. The gap between 0200 and 0230 UT is a period when bright stars over the limb of the earth are within the UVI field of view. The PCN model, with no knowledge of look direction, is
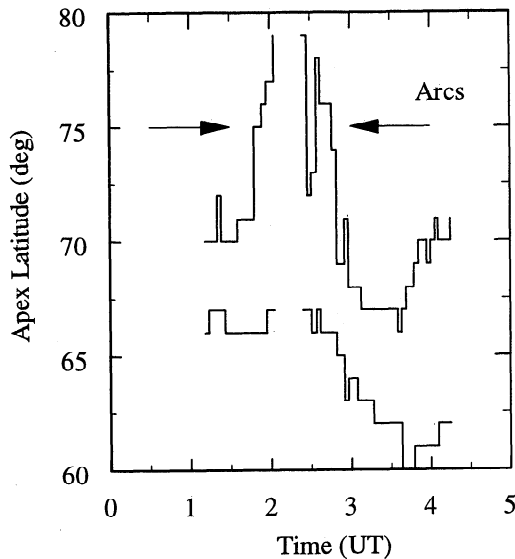
Figure 2. Equatorward and poleward boundaries for the midnight sector (21 - 03 MLT). The region between 2.5 and 3.0 UT is dominated by transpolar arcs that distort the poleward boundary determinations during this period.

mislead by the bright stars and incorrectly identifies the oval during these periods.

Figure 3 shows the areas of both the oval and cap regions. The cap area is identified as being the area northward of the poleward boundary. Consequently it is not affected by the transpolar arcs except in the sense that the poleward boundary is perturbed by the arcs. The oval area, however, is based on the pixels identified by the PCN model. This recognizes that the oval is not necessarily a contiguous region of emissions but is made up of
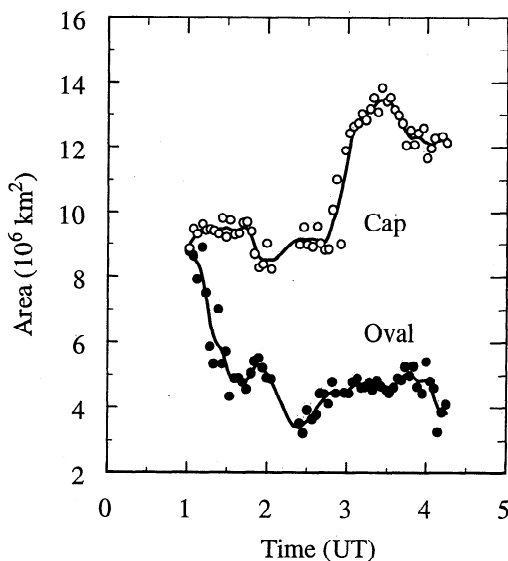

Figure 3. Areas of both the auroral oval and the polar cap. The cap area is defined as being the region northward of the poleward boundaries shown in Figure 1. The oval area is defined as being the summed pixel areas as identified by the PCN model. Uncertainties in the area estimation are principally due to uncertainties in instrument pointing and vary across the field of view. The uncertainties from these sources are less than 5%.

discrete emission areas. For example, after 0415 UT a distinct gap occurs near midnight. This area is excluded from the oval area estimate. On the other hand, no attempt is made to isolate the pixels within the transpolar arcs from those in the main oval. Note that this is significant only during the period of transpolar arc development between 0200 and 0300 UT. The entire oval is within the UVI field of view until 0415 UT when the dayside boundary begins to be clipped. This affects only the final two UVI observations.

The polar cap area increased with the initial impact of the shock and reached a local maximum at about 0130 UT. This initial increase is due to the increase of the solar wind pressure and occurred while the IMF was in the northward direction (Figure 4). (There is a delay of 12 - 15 minutes from the IMF observation and the auroral response [*Spann et al., 1997*] due to propagation from the WIND location to the magnetopause.) The increase of the polar cap area which begins at about 0230 UT nearly coincides with the turning of the IMF Bz southward. Note that the polar cap continually increases as the IMF Bz remained negative. The cap area increases by 45% (4.3 x 10^6 km^2) and maximum area is reached at the onset of the substorm, which coincides with the turning of the IMF to the northward direction. Subsequently the polar cap size decreased by 16% while the IMF Bz remained in the northward direction. Recall that the entire oval region is viewed by UVI with the possible exception of the final two points which are slightly clipped on the dayside of the image. Even in these cases, however, UVI has a clear view of the poleward boundary throughout the auroral region. Hence the decrease in polar cap size after substorm onset cannot be attributed to a field of view effect.

The behavior of the auroral oval area is different. The arrival of the shock abruptly decreased the area reducing the size by about a factor of two in about 30 minutes. At 0150 UT a small increase is seen in the oval area that is matched by a similar decrease in cap area. This is the result of a brief activation that then evolved into one of the transpolar arcs attached near local midnight to the oval. After this feature faded a further decrease in size of the oval was observed with the minimum size occurring around 0230 UT. This corresponded to a total decrease by a factor of almost 3 over the course of 1.5 hours. Thereafter the oval area increased by 4.3 x 10^6 km^2 between 0300 UT and the sub-
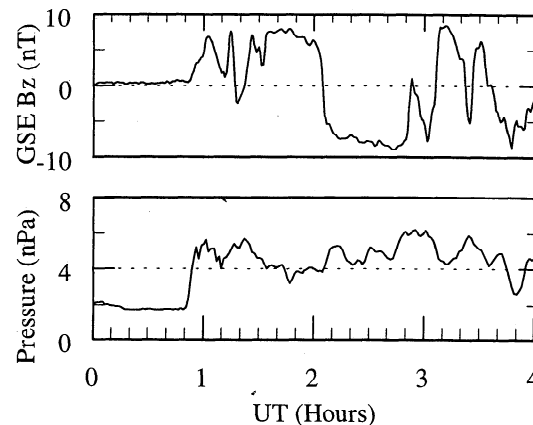

Figure 4. Interplanetary magnetic field and density measured by the WIND spacecraft located at 85 XGSE, -59 YGSE, -3 ZGSE for January 10th, 1997 from 0 UT to 4 UT. Adapted from *Spann et al.* [1997].

storm onset (0334 UT). A small but noticeable increase of the area was observed with the substorm onset.

Discussion

The principal contribution of this study is the analysis that follows from unprecedented opportunity to follow the morphological response of the aurora to a magnetic storm, observing the auroral behavior from the initial contact with the solar shock front to substorm onset over three hours later. The UVI data allows analysis at excellent temporal resolution and over a large dynamic range of intensities and morphological forms, including transpolar arc development, substorm growth phase, and the expansive substorm onset.

UVI global auroral images show that the behavior of the auroral boundaries during the magnetic cloud event of January 10, 1997 is complex but systematic. The auroral morphology demonstrates a clear substorm growth phase characterized by equatorward motion of the auroral boundaries and increase in polar cap size followed by expansive substorm onset with rapid poleward motion of the auroral forms. With an assumed propagation delay on the order of 12 - 15 minutes from the upstream WIND observations, the growth and onset phases are coincident with southward and northward turnings, respectively, of the IMF Bz component. The observed correlation between the behavior of the IMF and the boundary area is extremely good with a response time within a few minutes as shown by the observations of the polar cap area that continuing to increase for the entire time interval of negative IMF Bz component, the area reaching a maximum at the substorm onset, and the area decreasing following the turning of Bz in the northward direction, and the continuing decrease of the area as the IMF Bz remained in the northward direction. Similar conclusions have been reached by *Makita et al.* [1985] and *Akasofu et al.* [1992]. (See also *Kamide et al.* [1997]).

The start of the substorm growth phase is identified by the equatorward motion of the lower latitude auroral boundaries in the midnight sector beginning at 0230 UT. Motion of the poleward boundaries is not as evident because of the complications from the transpolar arcs at this time. After the arcs have faded at 0300 UT the growth phase motion is evident in the poleward boundaries as well. This expansion of the auroral boundaries is reflected in an increase in cap area at the same time. The equatorward motion of the midnight sector is detectable for all magnetic local times between 1800 and 0600 MLT, but is strongest near local midnight. This MLT dependence is very similar to the results of previous observations of the motion of the poleward boundary [*Kamide et al.*, 1997]. The growth phase motion continues until substorm onset at 0334 UT. The equatorward boundary in the 24 MLT sector continues its expansion for several minutes after the beginning of poleward motion of the high latitude boundary.

The size of the polar cap is strongly correlated with the substorm phases. In contrast to the polar cap area, however, the total oval emission area shows relatively small response to the substorm phases. Furthermore, there is little evidence of trade off between oval and cap areas, i.e. a decrease in area of the polar cap is not explained by an increase in area of the oval. For example, between 0330 and 0400 UT the cap decreases by 2.5×10^6 km^2 while the expanding oval increases by only 7.7×10^5 km^2 at the same time. More dramatic differences are seen during the substorm growth phase and during the 1.5 hours after contact with the solar shock, when the oval size drops by a factor of 2.7 while the polar cap size, which began the period equal to the oval size, remains essentially unchanged.

References

Akasofu, S.-I., C.-I. Meng, , and K. Makita, Changes in the size of the open field line region during substorms, *Planet. Space Sci., 40,* 1513, 1992.

Blanchard, G. T., L. R. Lyons, and J. C. Samson, Accuracy of using 6300 Å auroral emission to identify the magnetic separatrix on the night side of Earth, *J. Geophys. Res., 102,* 9697, 1997.

Frank, L. A., and J. D. Craven, Imaging results from Dynamics Explorer 1, *Rev. Geophys., 26,* 249-284, 1988.

Kamide, Y., S. Kokubun, L. F. Bargatze, and L. A. Frank, The size of the polar cap as an indicator of substorm energy, *Phys. Chem. Earth,* in press, 1997.

Makita, K., C.-I. Meng, and S.-I. Akasofu, Temporal and spatial variations of the polar cap dimension inferred from the precipitation boundaries, *J. Geophys. Res., 90,* 2744, 1985.

Murphree, J. S., R. D. Elphinstone, L. L. Cogger, and D. Hearn, Viking optical substorm signatures, *Magnetospheric Substorms, Geophys. Monogr. Ser., 64,* edited by J. R. Kan, Thomas A. Potemra, S. Kokubun, T. Iijima, 1991.

Newell, P. T., S. Wing, C.-I. Meng, and V. Sigillito, The auroral position, structure, and intensity of precipitation from 1984 onward: An automated on-line data base, *J. Geophys. Res., 96,* 5877, 1991.

Ranganath, H. S., and G. Kuntimad, Image Segmentation using Pulse Coupled Neural Networks, *Proc. of Intl. Conf. on Neural Networks,* Orlando, FL, June-July 1994, 1285-1290.

Spann, Jr., J. F., M. Brittnacher, R. Elsen, G. A. Germany, and G. K. Parks, Initial response of the aurora to the January 10, 1997 magnetic cloud, *Geophysical Research Letters,* in press, 1998.

Torr, M. R., D. G. Torr, M. Zukic, R. B. Johnson, J. Ajello, P. Banks, K. Clark, K. Cole, C. Keffer, G. Parks, B. Tsurutani, J. Spann, A far ultraviolet imager for the International Solar-Terrestrial physics mission, *Space Sci. Rev., 71,* 329, 1995.

M. Brittnacher, R. Elsen, and G. Parks, Geophysics Program, Box 351650, University of Washington, Seattle WA 98195.

G. Germany and W. Swift, Center for Space Plasma and Aeronomic Research, TH S131, University of Alabama in Huntsville, AL 35899 (e-mail: germanyg@cspar.uah.edu).

H. Ranganath and P. Richards, Computer Science Department, University of Alabama in Huntsville, AL 35899.

J. Spann, Space Science Laboratory, NASA Mail Code ES83, NASA Marshall Space Flight Center, Huntsville AL 35812.